A Methodology for Analysis of Fluid Structure Interaction Accounting for Free Surface Waves

E. Oñate
J. García

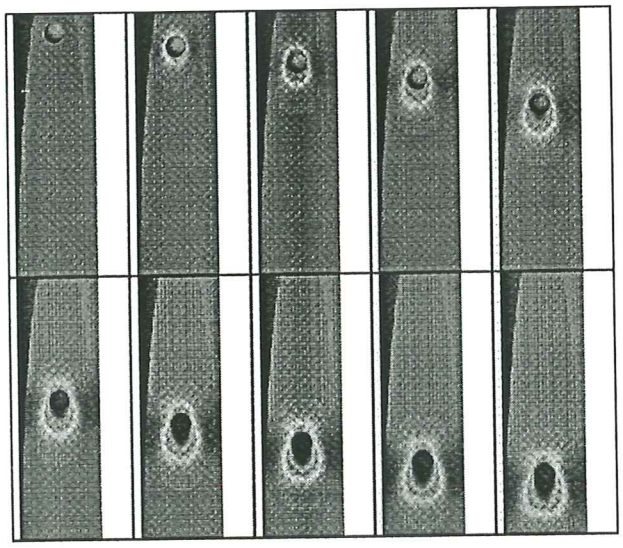

Publication CIMNE Nº 166, Juny 1999

A Methodology for Analysis of Fluid Structure Interaction Accounting for Free Surface Waves

E. Oñate
J. García

Publication CIMNE Nº 166, Juny 1999

International Center for Numerical Methods in Engineering
Gran Capitán s/n, 08034 Barcelona, Spain

Abstract. *A stabilized semi-implicit frictional step finite element method for solving coupled fluid-structure interaction problems involving free surface waves is presented. The stabilized equations are derived at a differential level via a finite element calculus procedure. A new mesh updating technique based on solving a fictitious elastic problem on the moving mesh is described. One example of the efficiency of the stabilized semi-implicit algorithm for the coupled solution of fluid-structure interaction problems is presented.*

1 Introduction

Accurate prediction of the fluid-structure interaction effects for a totally or partially submerged body in a flowing liquid including a free surface is a problem if great relevance in offshore engineering and naval architecture among many other fields.

The difficulties in accurately solving the coupled fluid-structure interaction problem in this case are mainly due to the following reasons:

1. The difficulty of solving numerically the incompressible fluid dynamic equations which typically include intrinsic non linearities except for the simplest and limited potential flow model.

2. The obstacles in solving the constraint equation stating that at the free surface boundary the fluid particles remain on that surface which position is in turn unknown.

3. The difficulties in solving the problem of motion of the submerged body due to the interaction forces while minimizing the distorsion of the finite elements discretizing the fluid domain thus reducing the need of remeshing.

This paper extends recent work of the authors [1] to derive a stabilized finite element method which allows to overcome above three obstacles. The starting point are the modified governing differential equations for the incompressible viscous flow and the free surface condition incorporating the necessary stabilization terms via a *finite increment calculus* (FIC) procedure developed by the authors [2–6]. The FIC approach has been successfully applied to the finite element and meshless solution of a range of advective-diffusive transport and fluid flow problems [1–6].

The modified governing equations are written in an arbitrary lagrangian-eulerian (ALE) form to account for the effect of relative movement between the mesh and the fluid points. These equations are solved in space-time using a semi-implicit fractional step approach and the finite element method (FEM). Free surface wave effects are accounted for via the introduction of a prescribed pressure at the free surface computed from the wave height.

The movement of the submerged body within the fluid due to the interaction forces is treated by solving a structural dynamic problem using the fluid forces as input loads. A

method to update the mesh for the fluid domain following the movement of the submerged body which minimizes element distorsion is presented. The mesh update procedure is based on the iterative finite element solution of a linear elastic problem on the mesh domain where fictitions elastic properties are assigned so that elements suffering higher movements are stiffer [8].

The content of the paper is structured as follows. First details of the stabilized semi-implicit fractional step approach using the FEM is described. Next the mesh updating procedure is presented. Finally some examples of a coupled fluid-interaction problem are given.

2 Stabilized finite element formulation for the fluid flow equations

We consider the motion around a body of a viscous incompressible fluid including a free surface.

The stabilized form of the governing differential equations for the three dimensional (3D) problem can be written in ALE form as

Momentum

$$r_{m_i} - \underline{\frac{1}{2} h_{mj} \frac{\partial r_{m_i}}{\partial x_j}} = 0 \qquad \text{on } \Omega \quad i,j = 1,2,3 \tag{1}$$

Mass balance

$$r_d - \underline{\frac{1}{2} h_{dj} \frac{\partial r_d}{\partial x_j}} = 0 \qquad \text{on } \Omega \quad j = 1,2,3 \tag{2}$$

Free surface

$$r_\beta - \underline{\frac{1}{2} h_{\beta_j} \frac{\partial r_\beta}{\partial x_j}} = 0 \qquad \text{on } \Gamma_\beta \quad j = 1,2 \tag{3}$$

where

$$r_{m_i} = \rho \left[\frac{\partial u_i}{\partial t} + \frac{\partial}{\partial x_j}(v_i u_j) \right] + \frac{\partial p}{\partial x_i} - \frac{\partial \tau_{ij}}{\partial x_j} - b_i \tag{4}$$

$$r_d = \rho \frac{\partial u_i}{\partial x_i} \qquad i = 1,2,3 \tag{5}$$

$$r_\beta = \frac{\partial \beta}{\partial t} + v_i \frac{\partial \beta}{\partial x_i} - u_3 \qquad i = 1,2 \tag{6}$$

and

$$v_i = u_i - u_i^m \tag{7}$$

In above u_i is the velocity along the i-th global reference axis, u_i^m is the mesh velocity and v_i is the relative velocity between the moving mesh and the fluid point i, ρ is the (constant) density of the fluid, p is the pressure, β is the wave elevation, b_i are the body forces acting in the fluid and τ_{ij} are the viscous stresses related to the viscosity μ by the standard expression

$$\tau_{ij} = \mu \left(\frac{\partial u_i}{\partial x_j} + \frac{\partial u_j}{\partial x_i} - \delta_{ij} \frac{2}{3} \frac{\partial u_k}{\partial x_k} \right) \tag{8}$$

The underlined terms in eqs.(1)–(3) introduce the necessary stabilization for the approximated numerical solution.

The distances h_{mj}, h_{dj} and h_{β_j} are termed *characteristic lengths* and represent the dimensions of the finite domain where balance of momentum, mass and transport of fluid particles is enforced. Details of the derivation of eqs. (1)-(3) can be found in [2,7].

A more convenient form of equation (2) can be written by assuming $h_{dj} = -2\tau_d u_j$ where τ_d is an intrinsic time parameter. Under this assumption and using eq. (1) the stabilized form of the mass balance equation can be written as (neglecting high order terms) [7]

$$r_d - \tau_d \frac{\partial \bar{r}_{m_i}}{\partial x_i} = 0 \tag{9}$$

where

$$\bar{r}_{m_i} = \rho \left(\frac{\partial u_i}{\partial t} + v_j \frac{\partial u_i}{\partial x_j} \right) + \frac{\partial p}{\partial x_i} - \frac{\partial \tau_{ij}}{\partial x_j} \tag{10}$$

The boundary conditions for the stabilized problem are written as

$$n_j \tau_{ij} + t_i + \underline{\frac{1}{2} h_{mj} n_j r_{m_i}} = 0 \qquad \text{on } \Gamma_t \tag{11}$$

$$u_j - u_j^p = 0 \qquad \text{on } \Gamma_u \tag{12}$$

where n_j are the components of the unit normal vector to the boundary and t_i and u_j^p are prescribed tractions and displacements on the boundaries Γ_t and Γ_u, respectively. The underlined stabilized terms appearing in the Neumann boundary condition (11) are obtained via the FIC approach [2,7].

Eqs.(1–12) are the starting point for deriving a variety of stabilized numerical methods for solving the incompressible Navier-Stokes equations. It can be shown that a number of standard stabilized finite element methods allowing equal order interpolations for the velocity and pressure fields can be recovered from the modified form of the momentum and mass balance equations given above [7]. A semi-implicit fractional step finite element procedure for solution of eqs. (1)-(3) and (11), (12) is presented in next section.

Stabilized fractional step method

Let us discretize in time the stabilized momentum equation (1) as

$$\rho\left[\frac{u_i^{n+1}-u_i^n}{\Delta t}+\frac{\partial}{\partial x_j}(v_iu_j)^n\right]+\frac{\partial p^{n+1}}{\partial x_i}-\frac{\partial \tau_{ij}^n}{\partial x_j}-b_i^n-\frac{1}{2}h_{mj}\frac{\partial r_{m_i}^n}{\partial x_j}=0 \tag{13}$$

A fractional step method (also termed "segregation" or "splitting" procedure) can be simply derived by splitting eq. (13) as follows

$$u_i^* = u_i^n-\Delta t\left[\frac{\partial}{\partial x_j}(v_iu_j)-\frac{1}{\rho}\frac{\partial \tau_{ij}}{\partial x_j}-\frac{1}{\rho}b_i-\frac{1}{2\rho}h_{mj}\frac{\partial r_{m_i}^n}{\partial x_j}\right]^n \tag{14}$$

$$u_i^{n+1} = u_i^*-\frac{\Delta t}{\rho}\frac{\partial p^{n+1}}{\partial x_i} \tag{15}$$

Note that addition of eqs.(14) and (15) gives the original stabilized momentum equation (13).

Substitution of eq.(15) into eq.(9) gives after some algebra [7]

$$(\Delta t+\tau_d)\Delta p^{n+1}=\frac{\partial u_i^*}{\partial x_i}-\tau_d\frac{\partial g_i^n}{\partial x_i}=0 \tag{16}$$

where

$$g_i=\rho\left(\frac{\partial u_i}{\partial t}+v_j\frac{\partial u_i}{\partial x_j}\right)-\frac{\partial \tau_{ij}}{\partial x_j}-b_i \tag{17}$$

Standard fractional step procedures neglect the contribution from the terms involving τ_d in eq. (16). It can be shown that these terms have an additional stabilization effect which improves the numerical solution when the values of Δt are small.

The free surface wave equation (3) can be also discretized in time to give

$$\beta^{n+1}=\beta^n-\Delta t\left[v_i^{n+1}\frac{\partial \beta^n}{\partial x_i}-u_3^{n+1}-\frac{1}{2}h_{\beta j}\frac{\partial r_\beta^n}{\partial x_j}\right] \qquad i,j=1,2 \tag{18}$$

A typical solution in time includes the following steps.

Step 1. Solve explicitely for the so called fractional velocities u_i^* using eq. (14).

Step 2. Solve for the pressure field p^{n+1} solving the laplacian equation (16). The pressures at the free surface computed from step 6 below in the previous time step are used as boundary conditions for solution of eq.(16). Alternatively a zero pressure condition at the surface should be imposed if the mesh boundary nodes are updated and placed on the new free surface.

Step 3. Compute the velocity field u_i^{n+1} at the updated configuration for each mesh node using eq. (15)

Step 4. Compute the new position of the free surface elevation β^{n+1} in the fluid domain by using eq. (18).

Step 5. Compute the movement of the submerged body by solving the dynamic equations of motion in the body subjected to the pressure field p^{n+1} and the viscous stresses τ_{ij}^n.

Step 6. Compute the new position of mesh nodes $\mathbf{x}_j^{n+1}$ in the fluid domain by using the mesh update algorithm described in next section. The pressure in the free surface is obtained from Benouilli equation as

$$p^{n+1} = p^o + \rho g(\beta^{n+1} - \beta^o) \tag{19}$$

where β^o and p^o are reference values of the free surface elevation and the pressure respectively and g is the gravity constant.

As already mentioned the effect of changes in the free surface elevation can be introduced in the step 2 of the flow solution as a prescribed pressure acting on the free surface.

Equation (19) does not account for viscosity and rotational effects in the fluid. These effects are however negligible in the free surface transport process and the pressure given by eq. (19) is a good approximation. Note that if the mesh is deformed after each time step so that the nodes are placed at the position defined by β^{n+1}, the use of eq. (19) is not longer necessary and a zero pressure condition can be applied on the free surface when solving for p^{n+1} in step 2.

The accuracy of above transient solution process depends on the time step size which should satisfy stability criteria for the coupled solution. Indeed larger time steps can be used if the values at time n in above equations are computed at $n + 1/2$. The solution process becomes now implicit and an iteration loop within each time step is then required.

Finite element discretization

Space discretization is carried out using the finite element method [9]. The velocity and pressure fields are interpolated within each element in the standard finite element manner as

$$u_i = \sum_j N_{u_j} (\bar{u_i})_j \tag{20}$$

$$p_i = \sum_j N_{p_j} \bar{p}_j \tag{21}$$

where N_{u_j} and N_{p_j} are the shape functions interpolating the velocity and pressure fields, respectively and $(\cdot)$ denote nodal values.

Similarly the wave height is discretized as

$$\beta = \sum_j N_{\beta_j} \bar{\beta}_j \tag{22}$$

where N_{β_j} are shape functions defined over the nodes discretizing the free surface.

It is worth noting that the stabilized formulation described allows an equal order interpolation of velocities and pressure [7]. A linear interpolation over triangles (2D) and tetrahedra (3D) for both u_i and p is chosen in the examples shown in the paper. Similarly linear elements are chosen to interpolate β on the free surface mesh.

The discretized integral form is obtained by applying the standard Galerkin procedure to eqs.(14),(15),(16) and (18) and the boundary conditions (11) and (12). The resulting expressions follow the pattern given in [7].

3 Computation of the stabilization parameters

Accurate evaluation of the stabilization parameters is one of the crucial issues in stabilized methods. Most of existing methods use expressions which are direct extensions of the values obtained for the simplest 1D case. It is also usual to accept the so called SUPG assumption, i.e. to admit that vector $\mathbf{h}_m$ has the direction of the velocity field. This restriction leads to instabilities when sharp layers transversal to the velocity direction are present. This additional defficiency is then corrected by adding a "shock capturing" (SC) stabilization term [10].

Let us first assume for simplicity that the stabilization parameters for the mass balance equations are the same than those for the momentum equations. This implies

$$\mathbf{h}_m = \mathbf{h}_d \tag{23}$$

The problem remains now finding the value of the characteristic length vectors $\mathbf{h}_m$. Indeed, the components of $\mathbf{h}_m$ can introduce the necessary stabilization along the streamline and transversal directions to the flow. Excellent results have been obtained by the authors using linear triangles and tetrahedra and a different value of the characteristic length vector for each momentum equation defined by

$$\mathbf{h}_{m_i} = h_s \frac{\mathbf{u}}{|\mathbf{u}|} + h_{c_i} \frac{\nabla u_i}{|\nabla u_i|} \qquad i = 1, 2, 3 \text{ for 3D problems} \tag{24}$$

where h_s and h_{c_i} are the "streamline" and "shock capturing" contributions given by

$$h_s = \max(\mathbf{l}_j^T \mathbf{u})/|\mathbf{u}| \tag{25}$$

$$h_{c_i} = \max(\mathbf{l}_j^T \nabla u_i)/|\nabla u_i| \quad , \quad j = 1, n_s \tag{26}$$

where $\mathbf{l}_j$ are the vectors defining the element sides ($n_s = 3$ for triangles and $n_s = 6$ for tetrahedra).

An alternative method for computing vector $\mathbf{h}_m$ in a more consistent manner is explained next.

3.1 Computation of the stabilization parameters via a diminishing residual procedure

The idea of this technique first presented in [2] and tested in [2–6] for advective-diffusive problems is the following. Let us assume that a finite element solution for the velocity and pressure fields has been found for a given mesh. The residual of the momentum equation corresponding to this particular solution is

$$ {}^1\bar{r}_{m_i} = \bar{r}_{m_i} - \frac{1}{2} h_{m_j} \frac{\partial \bar{r}_{m_i}}{\partial x_j} \tag{27} $$

The average residual over an element can be defined as

$$ {}^1\bar{r}^{(e)}_{m_i} = \frac{1}{\Omega^{(e)}} \int_{\Omega^{(e)}} {}^1\bar{r}_{m_i} d\Omega \tag{28} $$

Let us assume now that an enhanced numerical solution has been found for the same mesh and the same approximation (i.e. neither the number of elements nor the element type have been changed). This enhanced solution could be based, for instance, in a superconvergent recovery of derivatives [11,12]. The element residual for the enhanced solution is denoted ${}^2\bar{r}^{(e)}_{m_i}$. As the element residuals must tend to zero, the following condition must be satisfied

$$ {}^1\bar{r}^{(e)}_{m_i} - {}^2\bar{r}^{(e)}_{m_i} \geq 0 \tag{29} $$

Above equation applies for ${}^1\bar{r}^{(e)}_{m_i} > 0$. Clearly for ${}^1\bar{r}^{(e)}_{m_i} < 0$ the inequality in eq. (29) should be changed to ≤ 0.

Eq. (29) provides a system of equations which unkowns are the characteristic length parameters. Substituting eq. (27) into (29) and appling the identity condition in eq. (29) gives

$$ \mathbf{h}^{(e)}_m = \mathbf{A}^{-1}\mathbf{f} \tag{30} $$

with

$$ A_{ij} = 2 \left[\frac{{}^2\partial \bar{r}^{(e)}_{m_i}}{\partial x_j} - \frac{{}^1\partial \bar{r}^{(e)}_{m_i}}{\partial x_j} \right] \tag{31} $$

$$ \tag{32} $$

$$ f_i = {}^2\bar{r}^{(e)}_{m_i} - {}^1\bar{r}^{(e)}_{m_i} \tag{33} $$

The following "adaptive" algorithm can be proposed for obtaining a stabilized solution:

1. Solve for numerical values of velocities and pressure for an initial value $\mathbf{h}_m^{(e)} = \mathbf{h}_o^{(e)}$. Compute ${}^1\bar{r}_{m_i}^{(e)}$.

2. Evaluate the enhanced velocity and pressure fields. Compute ${}^2\bar{r}_{m_i}^{(e)}$.

3. Compute the updated value of $\mathbf{h}_m^{(e)}$ using eq. (30).

4. Repeat (1)–(3) until a stable solution is found.

Above strategy can be naturally incorporated into a transient solution scheme where the value of $\mathbf{h}_m^{(e)}$ is updated after the solution for each time step has been found.

The assumption $\mathbf{h}_d = \mathbf{h}_m$ can be relaxed and an independent value of the characteristic length vector $\mathbf{h}_d$ for the mass balance equation can be found following a similar approach as described for computing $\mathbf{h}_m$. Further details can be found in [2–6] where this technique has been successfully tested for steady state and transient advective-diffusive problems.

4 A simple algorithm for stable updating of mesh nodes

Finite element solution of fluid-structure interaction problems usually requires the update of the analysis mesh as described in previous section. A typical example is the study of movement of an object within a flowing liquid where the fluid mesh needs to be continuously updated accordingly to the changes in position of the object due to the interaction forces.

Chiandussi, Bugeda and Oñate [8] have recently proposed a simple method for movement of mesh nodes ensuring minimum element distorsion. The method is based on the iterative solution of a fictitions linear elastic problem on the mesh domain. In order to minimize mesh deformation the "elastic" properties of each mesh element are appropiately selected so that elements suffering greater movements are stiffer. The basis of the method is given below.

Let us consider an elastic domain with homogeneous isotropic elastic properties characterized by the Young modulus $\bar{E}$ and the Poisson coefficient ν. Once a discretized finite element problem has been solved using, for instance, standard C_o linear triangles (in 2D) or linear tetraedra (in 3D), the principal stresses ${}^1\sigma_i$ at the center of each element are obtained as

$$ {}^1\sigma_i = \bar{E}[\varepsilon_i - \nu(\varepsilon_j + \varepsilon_k)] \qquad i,j = 1,2,3 \ \text{ for 3D} \tag{34} $$

where ε_i are the principal strains.

Let us assume now that a uniform strain field $\varepsilon_i = \bar{\varepsilon}$ throughout the mesh is sougth. The principal stresses are then given by

$$ {}^2\sigma_i = E\bar{\varepsilon}(1-2\nu) \qquad i = 1,2,3 \ \text{ for 3D} \tag{35} $$

where E is the unknown Young modulus for the element.

A number of criteria can be now used to find the value of E. The most effective approach found in [8] is to equal the element strain energies in both analysis. Thus

$$U_1 = {}^1\sigma_i\varepsilon_i = \bar{E}[(\varepsilon_1^2+\varepsilon_2^2+\varepsilon_3^2) - 2\nu(\varepsilon_1\varepsilon_2+\varepsilon_2\varepsilon_3+\varepsilon_1\varepsilon_3)] \tag{36}$$

$$U_2 = {}^2\sigma_i\varepsilon_i = 3E\bar{\varepsilon}^2(1-2\nu) \tag{37}$$

Equaling eqs.(19) and (20) gives the sought Young modulus E as

$$E = \frac{\bar{E}}{3\bar{\varepsilon}^2(1-2\nu)}[(\varepsilon_1^2+\varepsilon_2^2+\varepsilon_3^2) - 2\nu(\varepsilon_1\varepsilon_2+\varepsilon_2\varepsilon_3+\varepsilon_1\varepsilon_3)] \tag{38}$$

Note that the element Young modulus is proportional to the element deformation as desired. Also recall that both $\bar{E}$ and $\bar{\varepsilon}$ are constant for all elements in the mesh.

The solution process includes the following two steps.

Step 1. Consider the finite element mesh as a linear elastic solid with homogeneous material properties characterized by $\bar{E}$ and ν. Solve the corresponding elastic problem with imposed displacements at the mesh boundary. These displacements can be due to a prescribed motion of a body within a fluid, to changes in the shape of the domain in an optimum design problem, etc.

Step 2. Compute the principal strains and the values of the new Young modulus in each element using eq. (38) for a given value of $\bar{\varepsilon}$. Repeat the finite element solution of the linear elastic problem with prescribed boundary displacements using the new values of E for each element.

The movement of the mesh nodes obtained in the second step ensures a quasi uniform mesh distorsion. Further details on this method including other alternatives for evaluating the Young modulus E can be found in [8].

The previous algorithm for movement of mesh nodes is able to treat the movement of the mesh due to changes in position of fully submerged and semi-submerged bodies. Note however that if the floating body intersects the free surface, the changes in the analysis domain geometry can be very important. From one time step to other emersion or inmersion of significant parts of the body can occur.

A posible solution to this problem is to remesh the analysis domain. However for most problems, a mapping of the moving surfaces linked to mesh updating algorithm described above can avoid remeshing (Figure 1).

The surface mapping technique used in this work is based on transforming 3D curved surfaces into reference planes. This allows to compute within each plane the local (in-plane) coordinates of the nodes for the final surface mesh accordingly to the changes in the floating line. The final step is to transform back the local coordinates of the surface mesh in the reference plane to the final curved configuration which incorporates the new floating line.

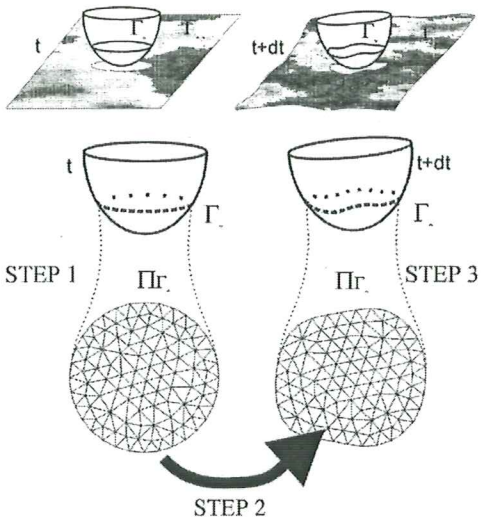

Figure 1: Changes in the fluid interface in a floating body

5 Examples

5.1 Example 1. Movement of a submerged sphere in an open channel

Figure 2 shows the geometry of the channel and the position of the sphere of 2m diameter with a weight of 1000 N and a rotational inertia of 1000 kgm^2. A mesh of 19870 linear tetrahedra with 4973 nodes has been used for the analysis.

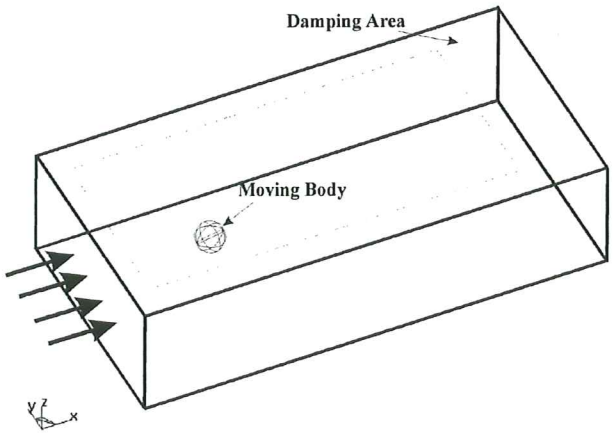

Figure 2: Geometry of the chanel with submerged sphere

The problem has been analyzed for values of Reynolds number = 200 and Froude number = 0.71 corresponding to a velocity of 1m/s at the inlet.

It is assumed that the sphere can only move vertically and rotate around the global y axes due to the forces induced by the fluid. The vertical displacement is constrained by a spring linking the sphere to the ground. An initial vertical velocity of 1m/s for the sphere has been taken.

Figure 3 shows a plot of the time evolution of the vertical displacement of the sphere. The contours of the velocity module in the fluid on two perpendicular planes at different times is shown in Figure 4. the deformation of the free surface at $t = 0.47$ s. and 3.16 s. is shown in Figure 5.

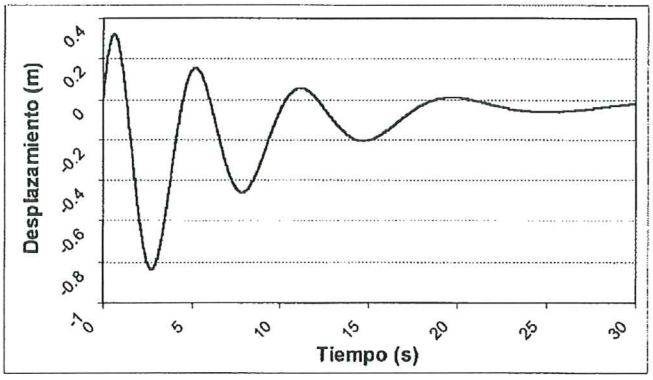

Figure 3: Time evolution of vertical displacement of sphere

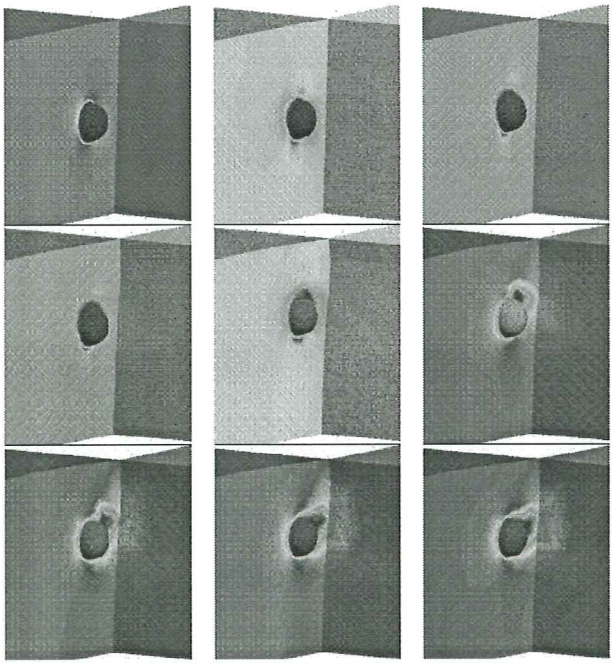

Figure 4: Contours of velocity module in the fluid on two perpendicular planes at different times

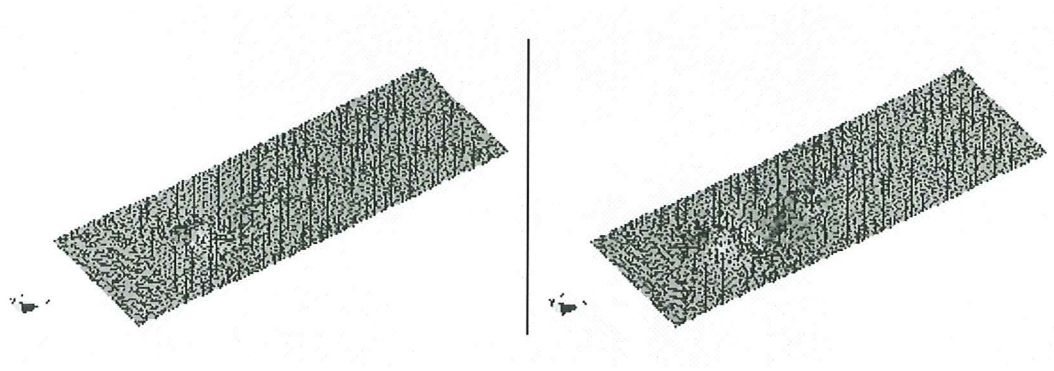

Figure 5: Deformation of the free surface amplified 10 times at times $t = 0.47$ s. and $t = 3.16$ s.

5.2 Example 2. Sphere falling in a tube filled with liquid

The movement of a sphere falling by gravity in a cylindrical tube filled with liquid is studied. The relationship between the diameters of the sphere and the tube is 1:4. The Reynolds number for the stationary speed is 100. The mesh has 85765 element with 13946 nodes.

Figures 6 and 7 show the contours of the mesh deformation and of the velocity in the domain for different times, respectively. The evolution of the falling speed is shown in Figure 8. Note the good agreement with the so called Stokes velocity computed by equaling the weight of the sphere with the resistance to the movement of the sphere expressed in terms of the velocity. Obviously, this value is slightly greater than the actual one as frictional effects are neglected.

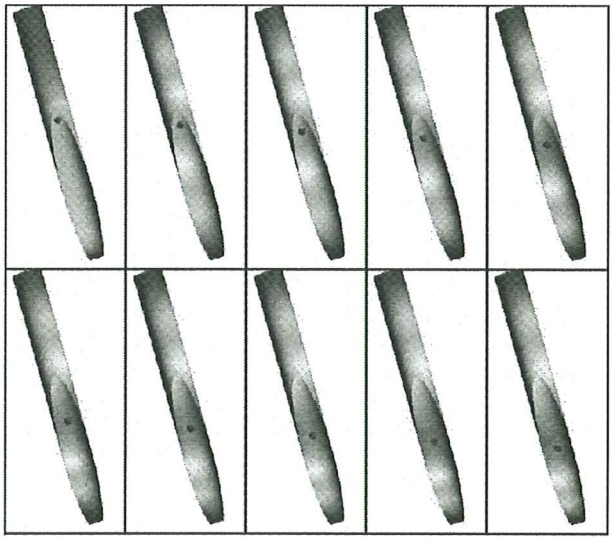

Figure 6: Following sphere. Contours indicate the evolution of the mesh deformation until stationary state is reached

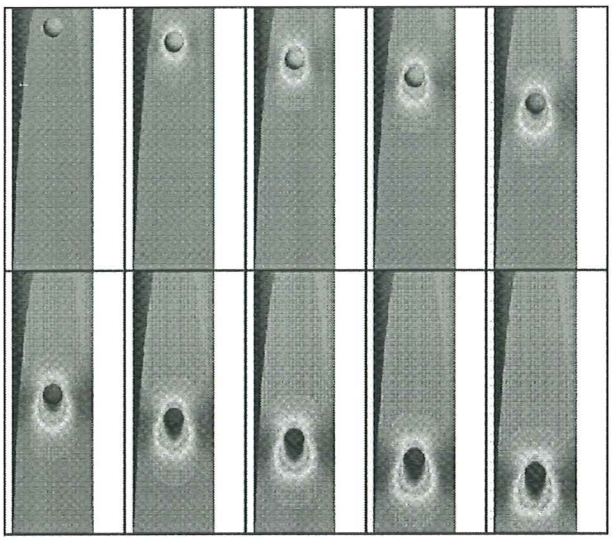

Figure 7: Falling sphere. Evolution of contours of the velocity module

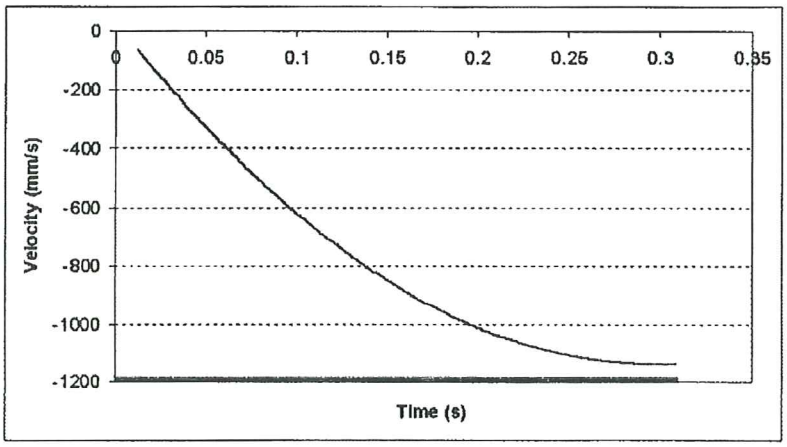

Figure 8: Falling sphere. Evolution of the falling speed. Straight line indicates the Stokes speed (1,195 m/s)

5.3 Example 3. Interactions of a rigid vertical cylinder with a moving stream

The definition of the problem is clearly seen in Figure 9. The cylinder diameter is 2 m and the stream speed is 1 m/s. The Froude and Reynolds numbers are 1.0 and 200, respectively. The walls of the cylinder are assumed to be rigid in this case. A mesh of 35567 tetrahedra and 4670 nodes is used for the analysis.

Figure 10 shows the contours of the velocity module and the vertical displacement in the mesh for a time $t = 4.57$ s. Note the important deformation of the free surface in this problem.

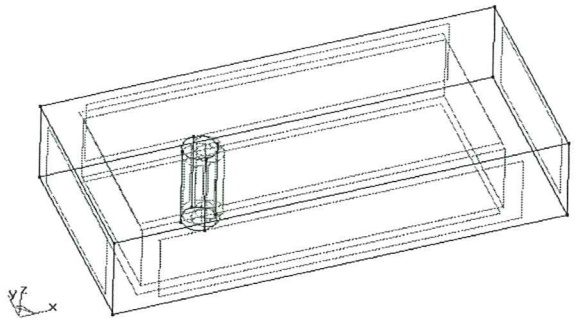

Figure 9: CAD definition of the vertical cylinder problem

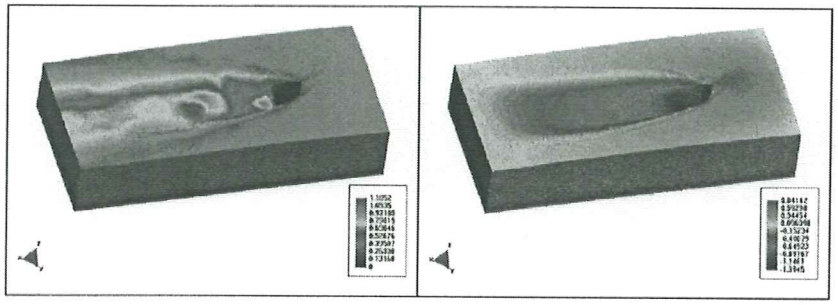

Figure 10: Vertical cylinder. Contours of velocity module and of vertical deformation of the mesh for $t = 4.57$ s.

6 Conclusions

A stabilized semi-implicit fractional step finite element method for analysis of coupled fluid-structure interaction problems involving free surface waves has been presented. The numerical method is based on a stabilized formulation using the finite increment calculus procedure for the Navier-Stokes equations [7] written in an ALE form. A procedure for automatic movement of mesh nodes during the coupled solution process has been developed. The method is adequate for solving large scale fluid-structure interaction situations in naval architecture and offshore engineering problems.

7 Acknowledgements

Support for this work was provided by the European Community through projects Brite-Euram BR 967-4342 SHEAKS and Esprit 24903 FLASH.

This support of Empresa Nacional BAZAN de Construcciones Navales y Militares, S.A. is also gratefully acknowledged.

Thanks are also given to Mr. J. Royo for his help in computing some of the examples presented.

References

[1] E. Oñate and J. García, A stabilized finite element method for analysis of fluid-structure interaction problems involving the surface waves, in *Computational Methods for Fluid-Structure Interaction*, T. Kvamsdal *et al.*, (Eds.), TAPIR Publishers, Norway, 1999.

[2] E. Oñate, Derivation of stabilized equations for advective-diffusive transport and fluid flow problems, *Comput. Meth. Appl. Mech. Engng.*, Vol. 151, 1-2, pp. 233–267, 1998.

[3] E. Oñate, J. García and S. Idelsohn Computation of the stabilization parameter for the finite element solution of advective-diffusive problems *Int. J. Num. Meth. Fluids*, Vol. 25, pp. 1385–1407, 1997.

[4] E. Oñate, J. García and S. Idelsohn, An alpha-adaptive approach for stabilized finite element solution of advective-diffusive problems with sharp gradients, *New Adv. in Adaptive Comp. Met. in Mech.*, P. Ladeveze and J.T. Oden (Eds.), Elsevier, 1998.

[5] E. Oñate and S. Idelsohn,, A mesh free finite point method for advective-diffusive transport and fluid flow problems,, *Computational Mechanics*, 21, 283–292, 1988.

[6] E. Oñate and M. Manzan, A general procedure for deriving stabilized space-time finite element methods for advective-diffusive problems, Publication PI-133, CIMNE, Barcelona, July 1998.

[7] E. Oñate, A finite element method for incompressible viscous flows using a finite increment calculus formulation, *Research Report* N. 150, CIMNE, Barcelona, January 1999.

[8] G. Chiandusi, G. Bugeda and E. Oñate, A simple method for update of finite element meshes, Research Report 147, CIMNE, Barcelona, January 1999.

[9] O.C. Zienkiewicz and R.C. Taylor, *The finite element method*, 4th Edition, Vol. 1, McGraw Hill, 1989, Vol. 2, McGraw Hill, 1991.

[10] R. Codina, A discontinuity-capturing crosswind dissipation for the finite element solution of the convection-diffusion equation, *Comput. Meth. Appl. Mech. Engng.*, Vol. **110**, pp. 325-342, 1993.

[11] O.C. Zienkiewicz and J.Z. Zhu, The superconvergent patch recovery (SPR) and adaptive finite element refinement, *Comput. Meth. Appl. Mech. Engng.*, Vol. **101**, pp. 207-224, 1992.

[12] N.E. Wiberg, F. Abdulwahab and X.D. Li, Error estimation and asdaptive procedures based on supercovergent patch recovery (SPR), *Archives of Comput. Meth. in Engng.*, Vol. **4**, 3, pp. 203-242, 1997.

ECCM '99
European Conference on
Computational Mechanics
August 31 – September 3
München, Germany

A METHODOLOGY FOR ANALYSIS OF FLUID STRUCTURE INTERACTION ACCOUNTING FOR FREE SURFACE WAVES

E. Oñate and J. García
International Centre for Numerical Methods in Engineering
Universidad Politécnica de Cataluña
Gran Capitán s/n, 08034 Barcelona, Spain
e–mail: cimne@etseccpb.upc.es

Informe de Investigación.
Portada: Fig. 7
en color: Mª Jesús.

Figure 3 shows a plot of the time evolution of the vertical displacement of the sphere. The contours of the velocity module in the fluid on two perpendicular planes at different times is shown in Figure 4. the deformation of the free surface at $t = 0.47$ s. and 3.16 s. is shown in Figure 5.

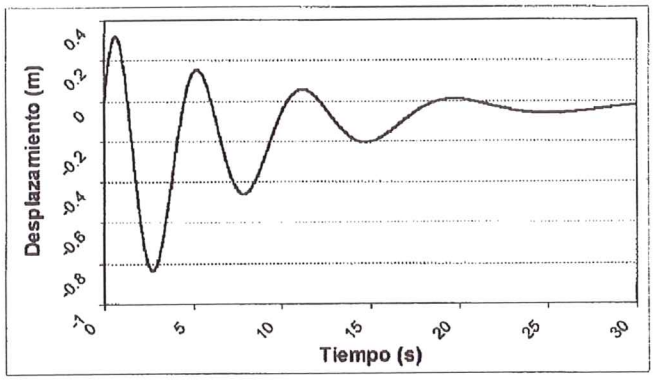

Figure 3: Time evolution of vertical displacement of sphere

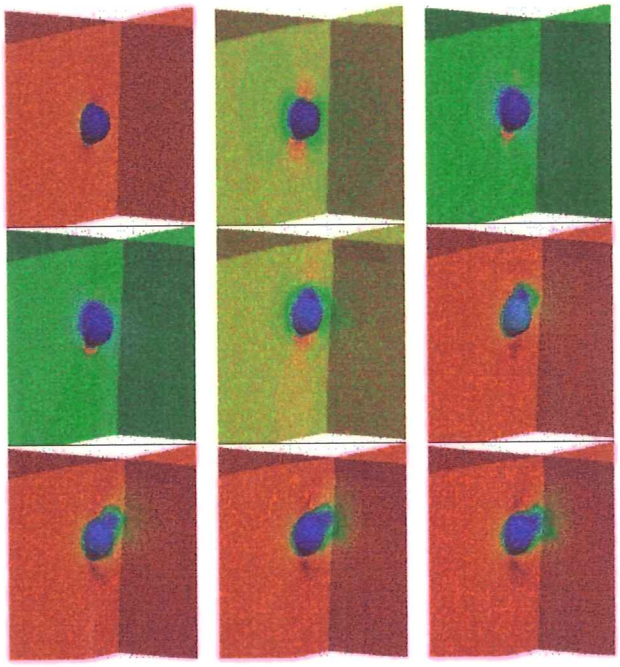

Figure 4: Contours of velocity module in the fluid on two perpendicular planes at different times

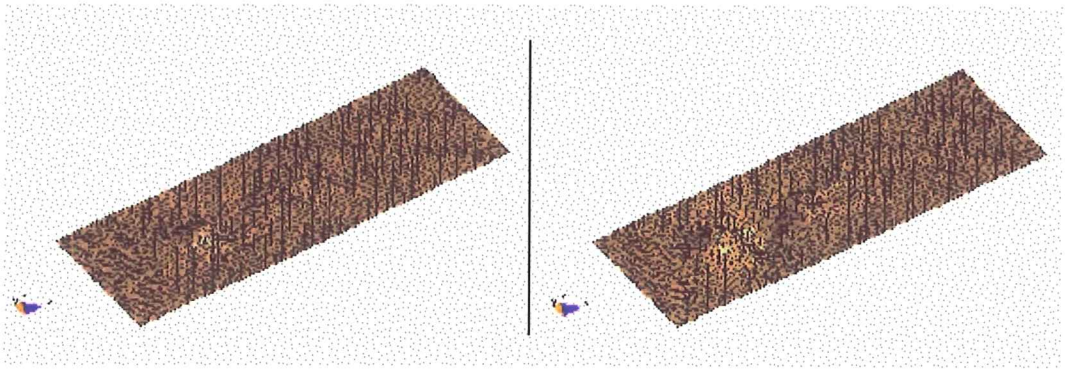

Figure 5: Deformation of the free surface amplified 10 times at times $t = 0.47$ s. and $t = 3.16$ s.

5.2 Example 2. Sphere falling in a tube filled with liquid

The movement of a sphere falling by gravity in a cylindrical tube filled with liquid is studied. The relationship between the diameters of the sphere and the tube is 1:4. The Reynolds number for the stationary speed is 100. The mesh has 85765 element with 13946 nodes.

Figures 6 and 7 show the contours of the mesh deformation and of the velocity in the domain for different times, respectively. The evolution of the falling speed is shown in Figure 8. Note the good agreement with the so called Stokes velocity computed by equaling the weight of the sphere with the resistance to the movement of the sphere expressed in terms of the velocity. Obviously, this value is slightly greater than the actual one as frictional effects are neglected.

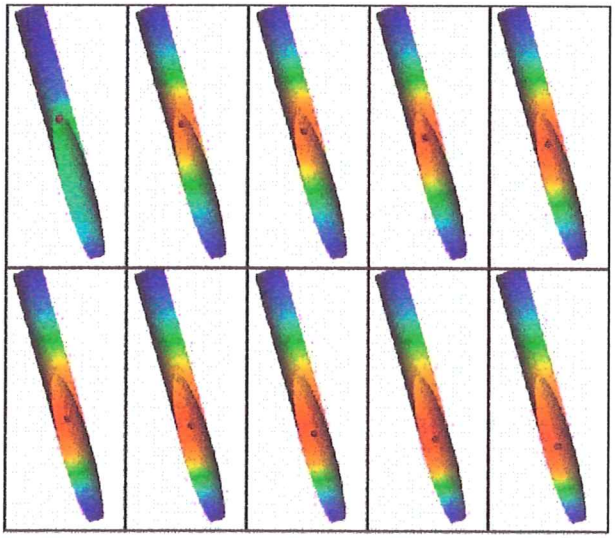

Figure 6: Following sphere. Contours indicate the evolution of the mesh deformation until stationary state is reached

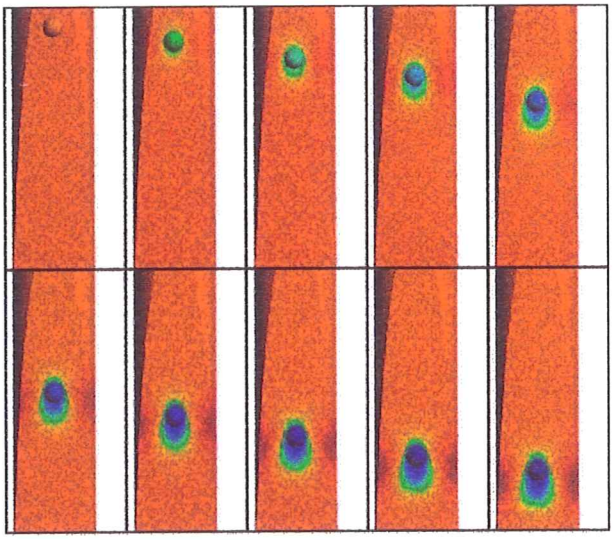

Figure 7: Falling sphere. Evolution of contours of the velocity module

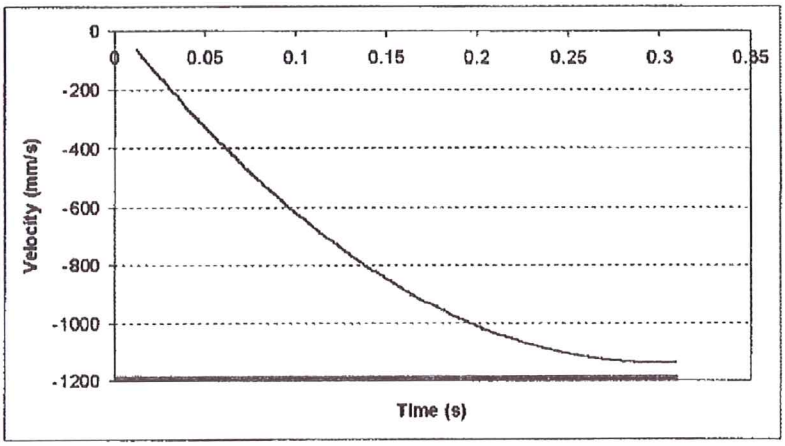

Figure 8: Falling sphere. Evolution of the falling speed. Straight line indicates the Stokes speed (1,195 m/s)

5.3 Example 3. Interactions of a rigid vertical cylinder with a moving stream

The definition of the problem is clearly seen in Figure 9. The cylinder diameter is 2 m and the stream speed is 1 m/s. The Froude and Reynolds numbers are 1.0 and 200, respectively. The walls of the cylinder are assumed to be rigid in this case. A mesh of 35567 tetrahedra and 4670 nodes is used for the analysis.

Figure 10 shows the contours of the velocity module and the vertical displacement in the mesh for a time $t = 4.57$ s. Note the important deformation of the free surface in this problem.

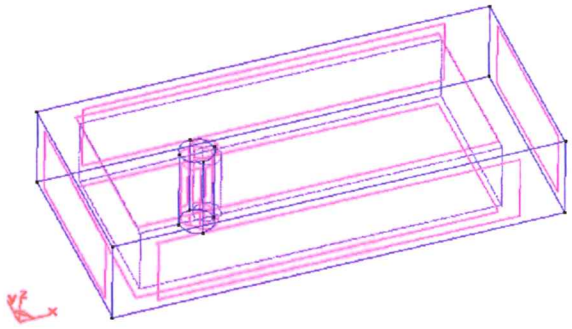

Figure 9: CAD definition of the vertical cylinder problem

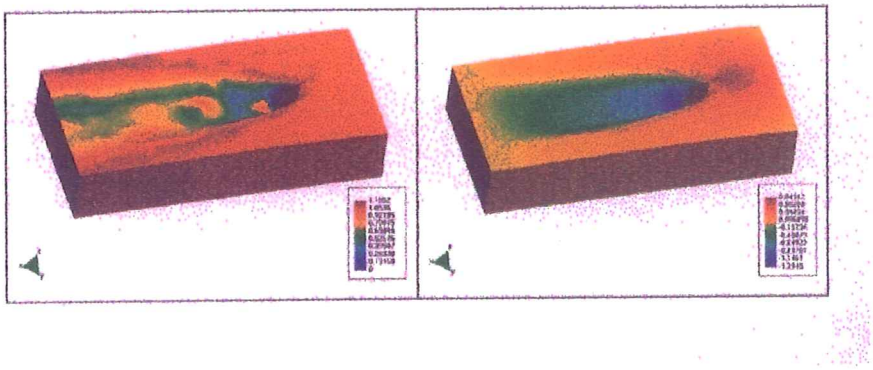

Figure 10: Vertical cylinder. Contours of velocity module and of vertical deformation of the mesh for $t = 4.57$ s.

6 Conclusions

A stabilized semi-implicit fractional step finite element method for analysis of coupled fluid-structure interaction problems involving free surface waves has been presented. The numerical method is based on a stabilized formulation using the finite increment calculus procedure for the Navier-Stokes equations [7] written in an ALE form. A procedure for automatic movement of mesh nodes during the coupled solution process has been developed. The method is adequate for solving large scale fluid-structure interaction situations in naval architecture and offshore engineering problems.

7 Acknowledgements

Support for this work was provided by the European Community through projects Brite-Euram BR 967-4342 SHEAKS and Esprit 24903 FLASH.

This support of Empresa Nacional BAZAN de Construcciones Navales y Militares, S.A. is also gratefully acknowledged.

Thanks are also given to Mr. J. Royo for his help in computing some of the examples presented.

INTERNATIONAL CENTER FOR NUMERICAL METHODS IN ENGINEERING

A Methodology for Analysis of Fluid Structure Interaction Accounting for Free Surface Waves

E. Oñate
J. García

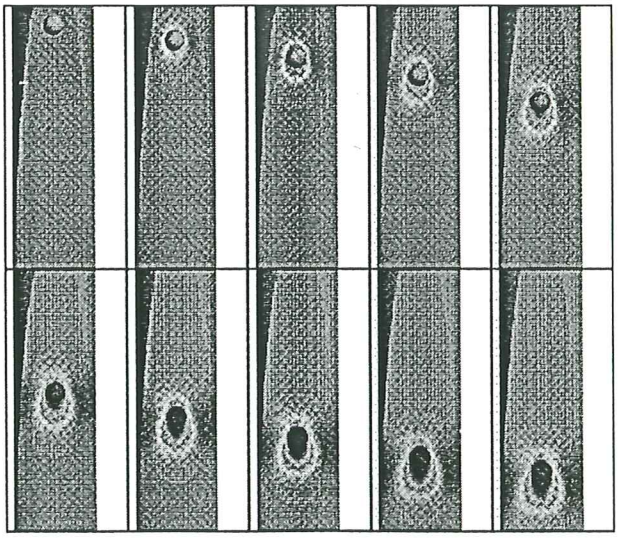

Publication CIMNE Nº 166, Juny 1999

A Methodology for Analysis of Fluid Structure Interaction Accounting for Free Surface Waves

E. Oñate
J. García

Publication CIMNE Nº 166, Juny 1999

International Center for Numerical Methods in Engineering
Gran Capitán s/n, 08034 Barcelona, Spain

Abstract. *A stabilized semi-implicit frictional step finite element method for solving coupled fluid-structure interaction problems involving free surface waves is presented. The stabilized equations are derived at a differential level via a finite element calculus procedure. A new mesh updating technique based on solving a fictitious elastic problem on the moving mesh is described. One example of the efficiency of the stabilized semi-implicit algorithm for the coupled solution of fluid-structure interaction problems is presented.*

1 Introduction

Accurate prediction of the fluid-structure interaction effects for a totally or partially submerged body in a flowing liquid including a free surface is a problem if great relevance in offshore engineering and naval architecture among many other fields.

The difficulties in accurately solving the coupled fluid-structure interaction problem in this case are mainly due to the following reasons:

1. The difficulty of solving numerically the incompressible fluid dynamic equations which typically include intrinsic non linearities except for the simplest and limited potential flow model.

2. The obstacles in solving the constraint equation stating that at the free surface boundary the fluid particles remain on that surface which position is in turn unknown.

3. The difficulties in solving the problem of motion of the submerged body due to the interaction forces while minimizing the distorsion of the finite elements discretizing the fluid domain thus reducing the need of remeshing.

This paper extends recent work of the authors [1] to derive a stabilized finite element method which allows to overcome above three obstacles. The starting point are the modified governing differential equations for the incompressible viscous flow and the free surface condition incorporating the necessary stabilization terms via a *finite increment calculus* (FIC) procedure developed by the authors [2–6]. The FIC approach has been successfully applied to the finite element and meshless solution of a range of advective-diffusive transport and fluid flow problems [1–6].

The modified governing equations are written in an arbitrary lagrangian-eulerian (ALE) form to account for the effect of relative movement between the mesh and the fluid points. These equations are solved in space-time using a semi-implicit fractional step approach and the finite element method (FEM). Free surface wave effects are accounted for via the introduction of a prescribed pressure at the free surface computed from the wave height.

The movement of the submerged body within the fluid due to the interaction forces is treated by solving a structural dynamic problem using the fluid forces as input loads. A

In above u_i is the velocity along the i-th global reference axis, u_i^m is the mesh velocity and v_i is the relative velocity between the moving mesh and the fluid point i, ρ is the (constant) density of the fluid, p is the pressure, β is the wave elevation, b_i are the body forces acting in the fluid and τ_{ij} are the viscous stresses related to the viscosity μ by the standard expression

$$\tau_{ij} = \mu \left(\frac{\partial u_i}{\partial x_j} + \frac{\partial u_j}{\partial x_i} - \delta_{ij} \frac{2}{3} \frac{\partial u_k}{\partial x_k} \right) \tag{8}$$

The underlined terms in eqs.(1)–(3) introduce the necessary stabilization for the approximated numerical solution.

The distances h_{mj}, h_{dj} and h_{β_j} are termed *characteristic lengths* and represent the dimensions of the finite domain where balance of momentum, mass and transport of fluid particles is enforced. Details of the derivation of eqs. (1)-(3) can be found in [2,7].

A more convenient form of equation (2) can be written by assuming $h_{dj} = -2\tau_d u_j$ where τ_d is an intrinsic time parameter. Under this assumption and using eq. (1) the stabilized form of the mass balance equation can be written as (neglecting high order terms) [7]

$$r_d - \tau_d \frac{\partial \bar{r}_{m_i}}{\partial x_i} = 0 \tag{9}$$

where

$$\bar{r}_{m_i} = \rho \left(\frac{\partial u_i}{\partial t} + v_j \frac{\partial u_i}{\partial x_j} \right) + \frac{\partial p}{\partial x_i} - \frac{\partial \tau_{ij}}{\partial x_j} \tag{10}$$

The boundary conditions for the stabilized problem are written as

$$n_j \tau_{ij} + t_i + \underline{\frac{1}{2} h_{mj} n_j r_{m_i}} = 0 \qquad \text{on } \Gamma_t \tag{11}$$

$$u_j - u_j^p = 0 \qquad \text{on } \Gamma_u \tag{12}$$

where n_j are the components of the unit normal vector to the boundary and t_i and u_j^p are prescribed tractions and displacements on the boundaries Γ_t and Γ_u, respectively. The underlined stabilized terms appearing in the Neumann boundary condition (11) are obtained via the FIC approach [2,7].

Eqs.(1–12) are the starting point for deriving a variety of stabilized numerical methods for solving the incompressible Navier-Stokes equations. It can be shown that a number of standard stabilized finite element methods allowing equal order interpolations for the velocity and pressure fields can be recovered from the modified form of the momentum and mass balance equations given above [7]. A semi-implicit fractional step finite element procedure for solution of eqs. (1)-(3) and (11), (12) is presented in next section.

Step 3. Compute the velocity field u_i^{n+1} at the updated configuration for each mesh node using eq. (15)

Step 4. Compute the new position of the free surface elevation β^{n+1} in the fluid domain by using eq. (18).

Step 5. Compute the movement of the submerged body by solving the dynamic equations of motion in the body subjected to the pressure field p^{n+1} and the viscous stresses τ_{ij}^n.

Step 6. Compute the new position of mesh nodes $\mathbf{x}_j^{n+1}$ in the fluid domain by using the mesh update algorithm described in next section. The pressure in the free surface is obtained from Benouilli equation as

$$p^{n+1} = p^o + \rho g(\beta^{n+1} - \beta^o) \tag{19}$$

where β^o and p^o are reference values of the free surface elevation and the pressure respectively and g is the gravity constant.

As already mentioned the effect of changes in the free surface elevation can be introduced in the step 2 of the flow solution as a prescribed pressure acting on the free surface.

Equation (19) does not account for viscosity and rotational effects in the fluid. These effects are however negligible in the free surface transport process and the pressure given by eq. (19) is a good approximation. Note that if the mesh is deformed after each time step so that the nodes are placed at the position defined by β^{n+1}, the use of eq. (19) is not longer necessary and a zero pressure condition can be applied on the free surface when solving for p^{n+1} in step 2.

The accuracy of above transient solution process depends on the time step size which should satisfy stability criteria for the coupled solution. Indeed larger time steps can be used if the values at time n in above equations are computed at $n + 1/2$. The solution process becomes now implicit and an iteration loop within each time step is then required.

Finite element discretization

Space discretization is carried out using the finite element method [9]. The velocity and pressure fields are interpolated within each element in the standard finite element manner as

$$u_i = \sum_j N_{u_j} (\bar{u_i})_j \tag{20}$$

$$p_i = \sum_j N_{p_j} \bar{p}_j \tag{21}$$

where N_{u_j} and N_{p_j} are the shape functions interpolating the velocity and pressure fields, respectively and $(\cdot)$ denote nodal values.

where $\mathbf{l}_j$ are the vectors defining the element sides ($n_s = 3$ for triangles and $n_s = 6$ for tetrahedra).

An alternative method for computing vector $\mathbf{h}_m$ in a more consistent manner is explained next.

3.1 Computation of the stabilization parameters via a diminishing residual procedure

The idea of this technique first presented in [2] and tested in [2–6] for advective-diffusive problems is the following. Let us assume that a finite element solution for the velocity and pressure fields has been found for a given mesh. The residual of the momentum equation corresponding to this particular solution is

$$ {}^1\bar{r}_{m_i} = \bar{r}_{m_i} - \frac{1}{2} h_{m_j} \frac{\partial \bar{r}_{m_i}}{\partial x_j} \tag{27} $$

The average residual over an element can be defined as

$$ {}^1\bar{r}^{(e)}_{m_i} = \frac{1}{\Omega^{(e)}} \int_{\Omega^{(e)}} {}^1\bar{r}_{m_i} d\Omega \tag{28} $$

Let us assume now that an enhanced numerical solution has been found for the same mesh and the same approximation (i.e. neither the number of elements nor the element type have been changed). This enhanced solution could be based, for instance, in a superconvergent recovery of derivatives [11,12]. The element residual for the enhanced solution is denoted ${}^2\bar{r}^{(e)}_{m_i}$. As the element residuals must tend to zero, the following condition must be satisfied

$$ {}^1\bar{r}^{(e)}_{m_i} - {}^2\bar{r}^{(e)}_{m_i} \geq 0 \tag{29} $$

Above equation applies for ${}^1\bar{r}^{(e)}_{m_i} > 0$. Clearly for ${}^1\bar{r}^{(e)}_{m_i} < 0$ the inequality in eq. (29) should be changed to ≤ 0.

Eq. (29) provides a system of equations which unkowns are the characteristic length parameters. Substituting eq. (27) into (29) and appling the identity condition in eq. (29) gives

$$ \mathbf{h}^{(e)}_m = \mathbf{A}^{-1}\mathbf{f} \tag{30} $$

with

$$ A_{ij} = 2 \left[\frac{{}^2\partial \bar{r}^{(e)}_{m_i}}{\partial x_j} - \frac{{}^1\partial \bar{r}^{(e)}_{m_i}}{\partial x_j} \right] \tag{31} $$

$$ \tag{32} $$

$$ f_i = {}^2\bar{r}^{(e)}_{m_i} - {}^1\bar{r}^{(e)}_{m_i} \tag{33} $$

The following "adaptive" algorithm can be proposed for obtaining a stabilized solution:

where E is the unknown Young modulus for the element.

A number of criteria can be now used to find the value of E. The most effective approach found in [8] is to equal the element strain energies in both analysis. Thus

$$U_1 = {}^1\sigma_i\varepsilon_i = \bar{E}[(\varepsilon_1^2+\varepsilon_2^2+\varepsilon_3^2) - 2\nu(\varepsilon_1\varepsilon_2+\varepsilon_2\varepsilon_3+\varepsilon_1\varepsilon_3)] \tag{36}$$

$$U_2 = {}^2\sigma_i\varepsilon_i = 3E\bar{\varepsilon}^2(1-2\nu) \tag{37}$$

Equaling eqs.(19) and (20) gives the sought Young modulus E as

$$E = \frac{\bar{E}}{3\bar{\varepsilon}^2(1-2\nu)}[(\varepsilon_1^2+\varepsilon_2^2+\varepsilon_3^2) - 2\nu(\varepsilon_1\varepsilon_2+\varepsilon_2\varepsilon_3+\varepsilon_1\varepsilon_3)] \tag{38}$$

Note that the element Young modulus is proportional to the element deformation as desired. Also recall that both $\bar{E}$ and $\bar{\varepsilon}$ are constant for all elements in the mesh.

The solution process includes the following two steps.

Step 1. Consider the finite element mesh as a linear elastic solid with homogeneous material properties characterized by $\bar{E}$ and ν. Solve the corresponding elastic problem with imposed displacements at the mesh boundary. These displacements can be due to a prescribed motion of a body within a fluid, to changes in the shape of the domain in an optimum design problem, etc.

Step 2. Compute the principal strains and the values of the new Young modulus in each element using eq. (38) for a given value of $\bar{\varepsilon}$. Repeat the finite element solution of the linear elastic problem with prescribed boundary displacements using the new values of E for each element.

The movement of the mesh nodes obtained in the second step ensures a quasi uniform mesh distorsion. Further details on this method including other alternatives for evaluating the Young modulus E can be found in [8].

The previous algorithm for movement of mesh nodes is able to treat the movement of the mesh due to changes in position of fully submerged and semi-submerged bodies. Note however that if the floating body intersects the free surface, the changes in the analysis domain geometry can be very important. From one time step to other emersion or inmersion of significant parts of the body can occur.

A posible solution to this problem is to remesh the analysis domain. However for most problems, a mapping of the moving surfaces linked to mesh updating algorithm described above can avoid remeshing (Figure 1).

The surface mapping technique used in this work is based on transforming 3D curved surfaces into reference planes. This allows to compute within each plane the local (in-plane) coordinates of the nodes for the final surface mesh accordingly to the changes in the floating line. The final step is to transform back the local coordinates of the surface mesh in the reference plane to the final curved configuration which incorporates the new floating line.

References

[1] E. Oñate and J. García, A stabilized finite element method for analysis of fluid-structure interaction problems involving the surface waves, in *Computational Methods for Fluid-Structure Interaction*, T. Kvamsdal *et al.*, (Eds.), TAPIR Publishers, Norway, 1999.

[2] E. Oñate, Derivation of stabilized equations for advective-diffusive transport and fluid flow problems, *Comput. Meth. Appl. Mech. Engng.*, Vol. 151, 1-2, pp. 233–267, 1998.

[3] E. Oñate, J. García and S. Idelsohn Computation of the stabilization parameter for the finite element solution of advective-diffusive problems *Int. J. Num. Meth. Fluids*, Vol. 25, pp. 1385–1407, 1997.

[4] E. Oñate, J. García and S. Idelsohn, An alpha-adaptive approach for stabilized finite element solution of advective-diffusive problems with sharp gradients, *New Adv. in Adaptive Comp. Met. in Mech.*, P. Ladeveze and J.T. Oden (Eds.), Elsevier, 1998.

[5] E. Oñate and S. Idelsohn,, A mesh free finite point method for advective-diffusive transport and fluid flow problems,, *Computational Mechanics*, 21, 283–292, 1988.

[6] E. Oñate and M. Manzan, A general procedure for deriving stabilized space-time finite element methods for advective-diffusive problems, Publication PI-133, CIMNE, Barcelona, July 1998.

[7] E. Oñate, A finite element method for incompressible viscous flows using a finite increment calculus formulation, *Research Report* N. 150, CIMNE, Barcelona, January 1999.

[8] G. Chiandusi, G. Bugeda and E. Oñate, A simple method for update of finite element meshes, Research Report 147, CIMNE, Barcelona, January 1999.

[9] O.C. Zienkiewicz and R.C. Taylor, *The finite element method*, 4th Edition, Vol. 1, McGraw Hill, 1989, Vol. 2, McGraw Hill, 1991.

[10] R. Codina, A discontinuity-capturing crosswind dissipation for the finite element solution of the convection-diffusion equation, *Comput. Meth. Appl. Mech. Engng.*, Vol. **110**, pp. 325-342, 1993.

[11] O.C. Zienkiewicz and J.Z. Zhu, The superconvergent patch recovery (SPR) and adaptive finite element refinement, *Comput. Meth. Appl. Mech. Engng.*, Vol. **101**, pp. 207-224, 1992.

[12] N.E. Wiberg, F. Abdulwahab and X.D. Li, Error estimation and asdaptive procedures based on supercovergent patch recovery (SPR), *Archives of Comput. Meth. in Engng.*, Vol. **4**, 3, pp. 203-242, 1997.